SANDIA REPORT

SAND2005-5709
Unlimited Release
Printed October 2005

Terahertz Time-Domain Spectroscopy of Atmospheric Water Vapor From 0.4 to 2.7 THz

Robert J. Foltynowicz and Ronald E. Allman

Approved for public release; further dissemination unlimited.

⊞ Sandia National Laboratories

Terahertz Time-Domain Spectroscopy of Atmospheric Water Vapor From 0.4 to 2.7 THz

R. J. Foltynowicz and R. E. Allman
Laser, Optics and Remote Sensing Department
Sandia National Laboratories
P.O. Box 5800 MS 1423
Albuquerque, NM 87185-1423

Abstract

We conducted broadband absorption measurements of atmospheric water vapor in the ground state, X ^{1}A$_1$ (000), from 0.4 to 2.7 THz with a pressure broadening-limited resolution of 6.2 GHz using pulsed, terahertz time-domain spectroscopy (THz-TDS). We measured a total of seventy-two absorption lines and forty-nine lines were identified as H$_2^{16}$O resonances. All the H$_2^{16}$O lines identified were confirmed by comparing their center frequencies to experimental values available in the literature.

Acknowledgements

Contents

Figures

Tables

Introduction

Water is the archetypal light, asymmetric top rotor displaying vast spectral complexity despite its deceivingly simple geometric form. It has been the center of intense spectroscopic investigations and theoretical model development since the 1930's and is still being studied today with the application of new spectroscopic measuring tools [1]. Historically, measuring water spectra had been known to be difficult in the microwave and submillimeter wavelength ranges. This difficulty stems from water's intrinsically large rotational constants which cause large frequency separations between transitions. To obtain an adequate spectrum for any type of analysis, one needs to scan a large bandwidth of frequencies which is challenging with high-resolution microwave and submillimeter techniques. Despite the difficulties, water vapor spectra have been measured by a large number of groups from 0.150 to 20.8 THz utilizing both microwave and Fourier techniques dating from 1962 to 1976 [2]. In 1978, Kauppinen et al. were the first to measure and catalog a pure rotational spectrum of water and its natural occurring isotopes $H_2^{17}O$, $H_2^{18}O$ and $HD^{16}O$ from 0.900 to 21.6 THz using only one technique for the entire bandwidth, a Michelson-type, double-beam Fourier spectrometer with a resolution of 540 MHz [2]. Utilizing Kauppinen's infrared data combined with their own microwave measurements of water from 0.022 to 0.988 THz, Messer and DeLucia conducted theoretical calculations to fit the experimental lines and to determine the spectroscopic constants for ground state water vapor, $H_2^{16}O$ [3]. They calculated line positions from 0.022 to 24.813 THz based on Watson's reduced centrifugal distortion Hamiltonian [3]. A year later, Messer et al. measured the submillimeter spectroscopy of $HD^{16}O$ and D_2O and published spectroscopic constants for these molecules using the same theoretical model used for $H_2^{16}O$ [4]. It wasn't until 1989 that the difficulty in measuring a broadband spectrum in the microwave and submillimeter range was simplified. Martin van Exter et al. developed a new technique called pulsed, terahertz time-domain spectroscopy (THz-TDS) [5]. This technique involved integrating a newly developed high brightness, broadband THz source (bandwidth ~ 1.3 THz) based on a femtosecond laser-activated photoconductive switch into a time-domain spectrometer. This technique allowed broadband spectral measurements in the Far IR from 0.2 to 1.5 THz with the spectral resolution limited by the scan length. Moreover, this technique was more sensitive than any of the current microwave or FTIR bolometer detection schemes by a factor of a thousand [5]. The sensitivity of THz-TDS comes from its coherent, optical detection scheme that eliminated the THz radiation-containing, thermal background from the measurement [5]. Exter et al. applied this technique to measure the absorption spectrum of atmospheric water vapor. As a result, they made the most accurate measurements of the absorption cross sections of the nine strongest water lines from 0.2 to 1.45 THz with a spectral resolution of 5 GHz [5]. In the decade that followed the development of THz-TDS, high-resolution work continued on water and its isotopes utilizing tunable far IR and three-diode laser difference frequency mixing to refine the theoretical Hamiltonians for these species. Matsushima et al. measured high-resolution lines for $H_2^{16}O$, $H_2^{17}O$ and $H_2^{18}O$ from 0.5 to 5 THz using tunable far-infrared spectrometer (TuFIR) with an accuracy of 150 kHz and established a new set of spectroscopic constants for all three species using Watson's A-reduced Hamiltonian [6-7]. Chen et al. found the frequencies of seventeen new $H_2^{16}O$ lines of water vapor between 0.841 to 1.575 THz using a three-diode laser difference frequency spectrometer with a resolution of 250 KHz as well as using a non-

power series effective Hamiltonian to calculate the center frequencies of $H_2^{16}O$ [8]. In 2001, the application of THz-TDS to atmospheric water returned and Han et al. published a broadband water vapor spectrum from 1 to 14 THz to prove the feasibility of a new, ultra-broadband THz-TDS system from 30 GHz to 40 THz. However, no detailed analysis of the water lines observed was completed and the low scan resolution was not disclosed [9].

At the present time, THz-TDS on atmospheric water vapor is limited to nine assigned absorption lines between 0.2 - 1.5 THz and an unassigned, low-resolution spectrum from 1 to 14 THz. The goal of this work was to conduct atmospheric water vapor measurements utilizing THz-TDS to expand the experimentally measured bandwidth of Exter's [5] work and improve the resolution of Han's [9] work. In addition, this paper will provide a novice THz experimentalists not only with data to benchmark a newly built THz-TDS system, but also provides descriptions on parameters required to build a ZnTe-based THz-TDS spectrometer. Utilizing a ZnTe crystal-based, pulsed, THz-TDS spectrometer with an experimental resolution of 6.2 GHz and a spectral range from 0.4 to 2.7 THz, a total of seventy-two absorption lines were measured. We were able to only assign forty-nine lines to $H_2^{16}O$ and the rest were unassigned due to the complexity of the spectrum. All the identified lines were confirmed by comparing their center frequencies to experimental values in the literature.

Experimental

The atmospheric water vapor spectra were measured with a pulsed, THz-TDS spectrometer utilizing optical rectification and free space, electro-optic sampling for THz generation and detection, respectively. Figure 1 shows a diagram of the ZnTe crystal-based THz-TDS spectrometer used in this investigation. A mode-locked, Ti:Sapphire oscillator (Coherent Mira 900) with a 115 fs pulsewidth, 76 MHz repetition rate and centered at 800 nm is split into a high energy pump and low energy probe beam. The vertically-polarized, pump beam propagates through a delay line (Newport ILS150PP) with 0.5 um resolution and is focused onto a 10 x 10 x 0.9 mm thick <110> ZnTe crystal (eV Products) at normal incidence with an average power of 311 mW and a beam diameter of 500 um. The THz beam that is generated on the output face of the ZnTe crystal is collected and collimated by a 10 cm focal length, off-axis parabolic mirror with a 90 degree reflection angle. The THz beam traverses a path length of 94 cm and is focused onto a 10 x 10 x 0.9 mm thick <110> ZnTe crystal sensor. The low energy probe beam is vertically polarized and is focused to a beam diameter of 50 um as it co-propagates with the THz beam through the ZnTe crystal. The probe beam then experiences a polarization rotation directly proportional to the THz electric field strength. The polarization change is analyzed by allowing the probe beam to traverse through a ¼ waveplate oriented at 45 degrees. The polarization components are split by a Wollaston prism with a 10 degree divergence angle and the resulting split beam is weakly focused onto a large area balanced photoreceiver (New Focus Model 2307) with a gain setting of 10^5 V/A. The average probe optical power of each polarization component present at the balanced photodiode is 3.8 mW. The THz generation is modulated at 2.6 KHz and the differential signal is measured by a SRS Model 830 DSP lock in amplifier with an integration time of 300 ms and a low pass filter roll off of 12dB/Oct. The data acquisition is controlled by LabVIEW 6.0 on a desktop PC. In addition, the complete propagation path of

5

the THz beam was enclosed in a nitrogen purged environment to prevent the interaction of atmospheric water vapor with the THz beam during our reference scans.

Off Axis Parabolic Mirror **Off Axis Parabolic Mirror**
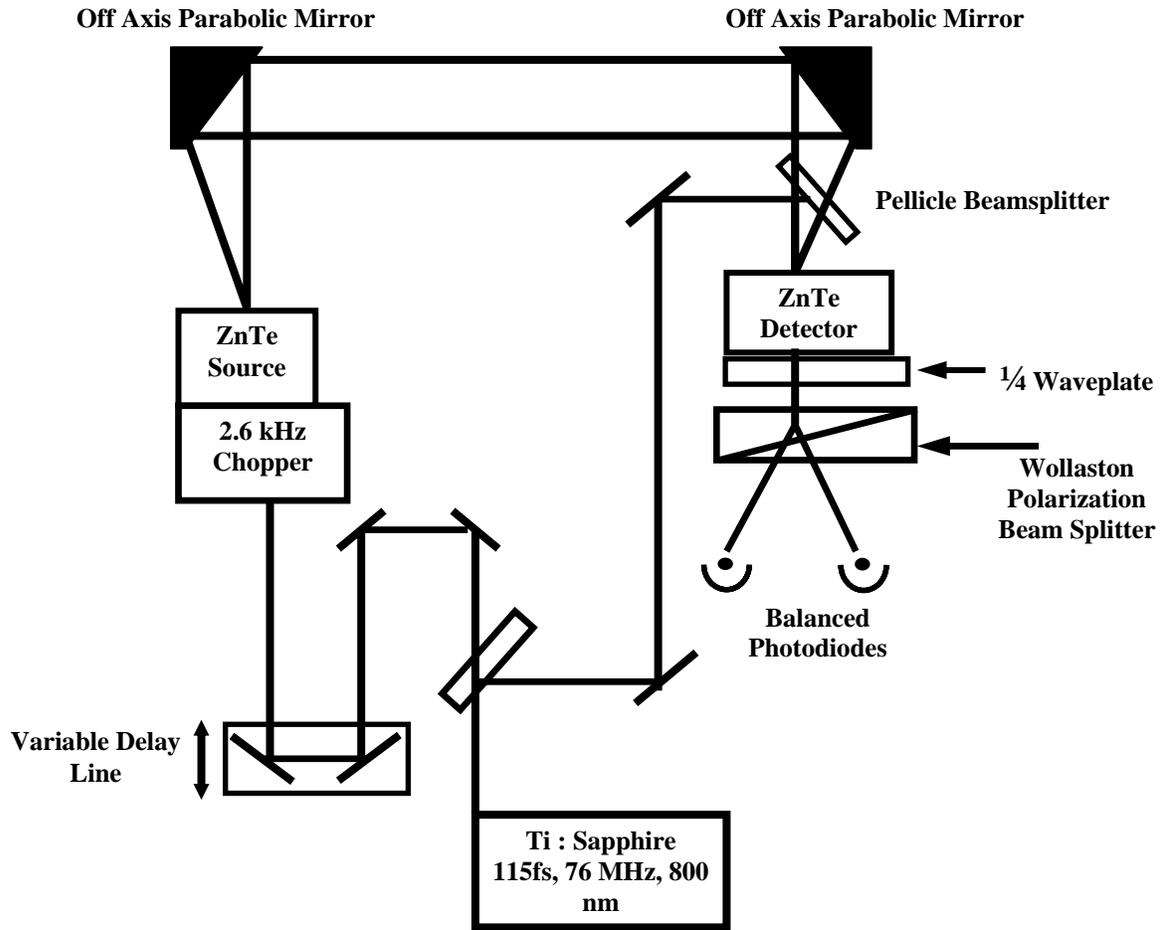
Figure 1 Terahertz time-domain spectroscopy spectrometer overview. A high energy, 115 fs pulse centered at 800 nm is split into a pump and probe beam. The pump beam interacts with a 0.9 mm thick, <110> ZnTe crystal to produce broadband THz radiation via optical rectification. The probe beam is used to analyze the THz field strength via free space electro-optic sampling utilizing a 0.9 mm thick, <110> ZnTe crystal.

Results

The experimental resolution for the measurements of atmospheric water vapor transitions is limited by the pressure broadening of the lines. Given that the atmospheric pressure in Albuquerque, New Mexico is 620 Torr and assuming a standard pressure broadening coefficient of 10 MHz / Torr, the pressure-broadening-limited resolution for our experiment is 6.2 GHz. Therefore, our experimental scan lengths are truncated at a 163 ps in the time-domain. Figure 2 shows an example of the time-domain profile of our *reference* scan.
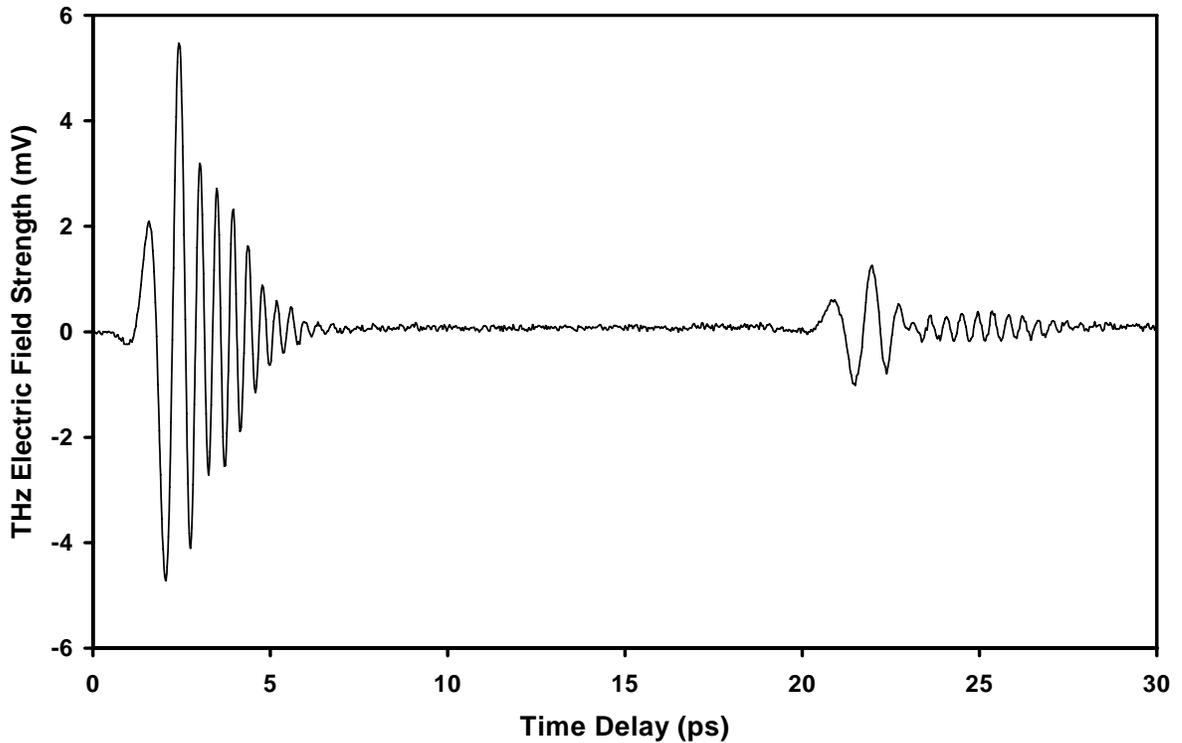
Figure 2. A typical time-domain profile of a nitrogen-rich environment with a relative humidity of 0 ±2% at 23.4 °C. This reference scan extends out to 163 ps, but only 30 ps are shown. No structure appears from 7 to 18 ps indicating no THz absorption or dispersion by water vapor molecules.

In this scan, the THz radiation is propagating through a nitrogen-rich environment with a relative humidity of 0 ±2% as measured with a hygrometer (Dickson TM325). The profile clearly shows a main THz pulse from 0 – 5 ps with a peak amplitude of approximately 6 mV and a secondary pulse with a peak at 20.5 ps. The peak at 20.5 ps is the weaker reflected pulse of the main THz beam as it propagated through two 0.9 mm thick ZnTe crystals. These reflections are reproducible and divide out in frequency space when we normalize the reference scan to the water vapor scan in our analysis. Also in Figure 2, note the signal directly after the main pulse (7 to 18 ps) shows a flat line devoid of structure or modulation which confirms that there is no interaction between the THz radiation and water vapor in the reference scan.

      The water vapor scan was taken by shutting off the nitrogen purge and exposing the THz beam to the atmosphere. We measured three absorption spectra for atmospheric water at three different times of the year. All three spectra were measured at a temperature of 23.4 °C, but two spectra had a relative humidity of 20 ±2 % (4.3 Torr of water vapor) and one spectrum had a relative humidity of 25 ± 2 % (5.4 Torr of water vapor). Figure 3 shows the time-domain profile for atmospheric water vapor with a relative humidity of 25 ±2 %.
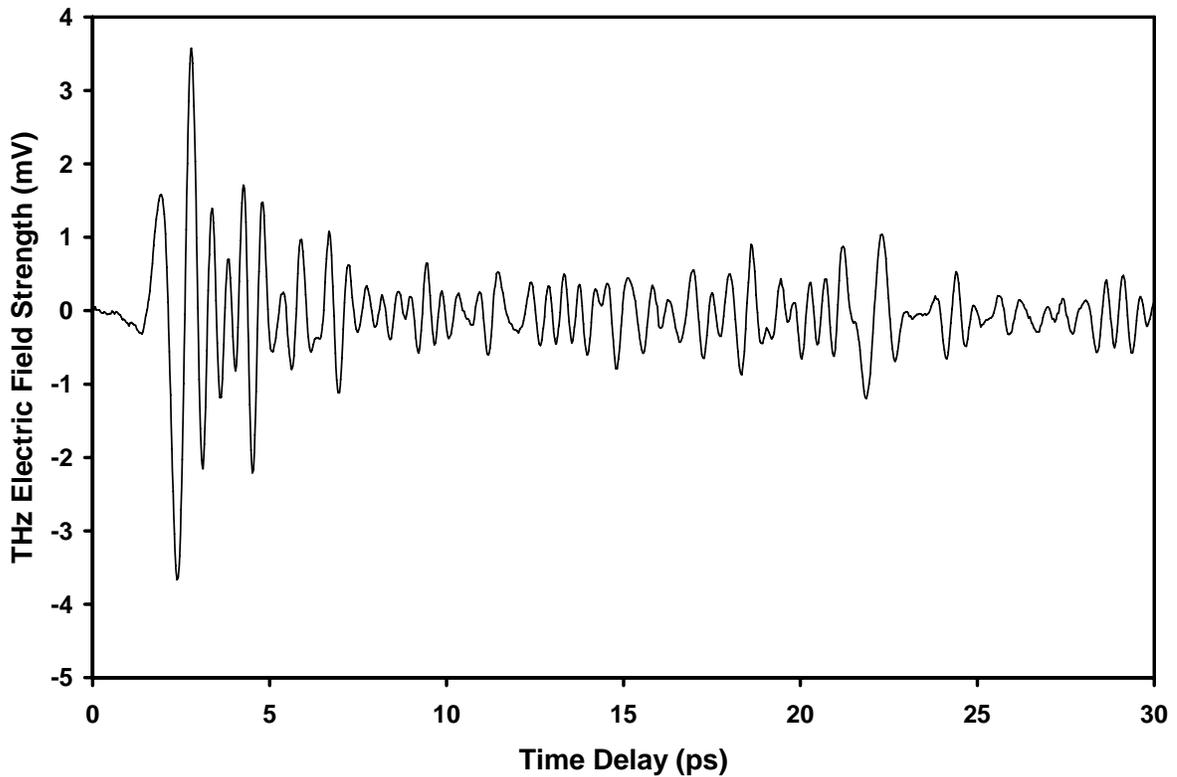
Figure 3. A time-domain profile of atmospheric water vapor with 25 ±2% relative humidity at 23.4 °C. This sample scan extends out to 163 ps, but only 30 ps are shown. Notice how the time-domain profile of the water vapor shows a dramatic change in the shape of the waveform due to the strong absorptions and dispersion of the THz radiation by water vapor molecules.

One can clearly see not only the reduction in the main pulse peak amplitude from approximately 6 mV to 3.5 mV when compared to the reference, but also the modulation of the THz waveform due to the absorption and dispersion of the THz beam when it interacted with water vapor in the 5 to 20 ps time frame. This occurs because the water vapor is creating phase and amplitude changes in the spectral components of the THz bandwidth that constructively and destructively interfere to produce a resultant waveform different from the reference.

 To obtain the absorption spectrum of the atmospheric water vapor, a FFT of the time-domain profiles for the reference and the sample scans was calculated. Since absorbance calculations are intensity based expressions, the resulting spectral amplitude profiles were squared to produce a power spectrum for both the reference and the water vapor scans. Finally, the Naperian absorbances were determined by taking the natural log of the ratio between the reference scan spectral power and the water vapor scan spectral power. Figure 4 shows the resulting absorption spectrum of atmospheric water vapor from 0.4 to 2.7 THz.
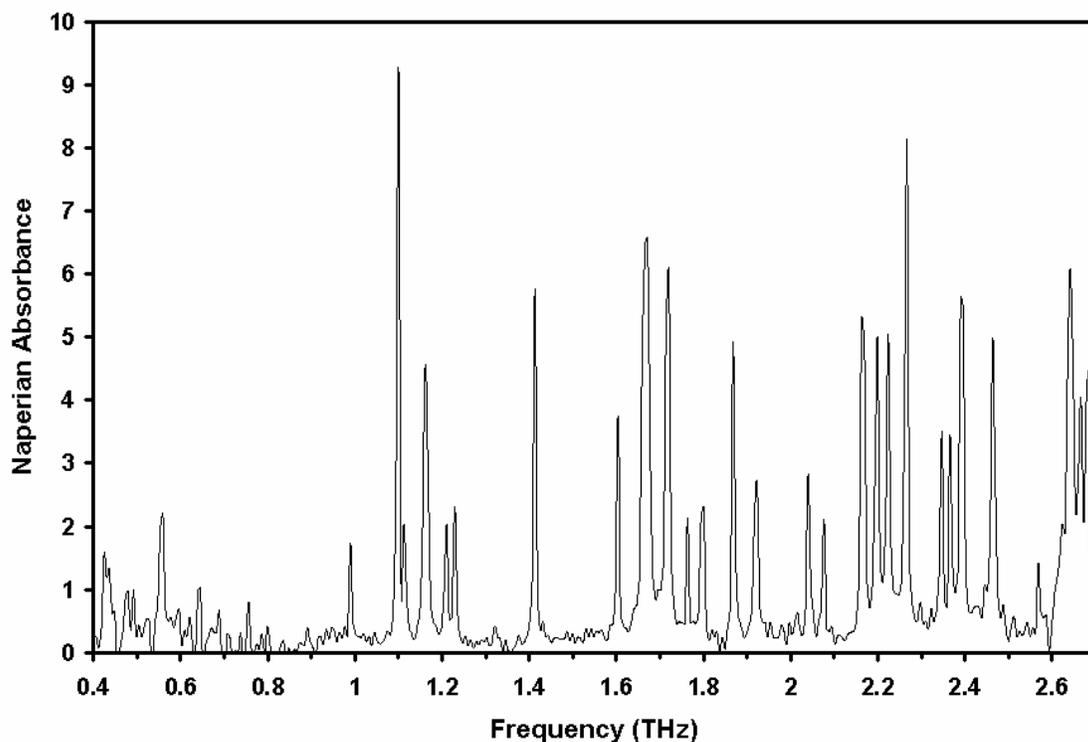
Figure 4. Measured absorption spectrum of atmospheric water vapor. The atmospheric pressure is 620 Torr with a relative humidity of 25 ±2% at 23.4 ^{o}C. The propagation length of the THz beam through the atmosphere is 94 cm.

Discussion

In order to measure the rotational absorption resonances of any molecule utilizing THz-TDS, the molecule must have a permanent dipole moment. Out of the most abundant molecules in the atmosphere which are diatomic nitrogen (78.08%), diatomic oxygen (20.95%), water vapor (0.03%), atomic argon (0.009%) and carbon dioxide (0.0003%), only water possesses a permanent dipole [10]. Since water is a bent, asymmetric top rotor with a C_{2V} symmetry point group, it has a permanent dipole moment with a magnitude of approximately two Debye [11]. Diatomic nitrogen, diatomic oxygen and carbon dioxide will not produce any rotational spectra because their linear symmetry prevents them from having a permanent dipole. Argon atoms, on the other hand, lack a moment of inertia and hence don't have any rotational motion that could produce rotational absorbances. By conducting pulsed, THz-TDS, the experiment itself acts as a filter to isolate the investigation of only the water vapor content in the atmosphere. However, not only will $H_2^{16}O$ be THz active, but also water's isotopes. The relative abundances of the isotopic water species in the atmosphere are approximately $H_2^{17}O$ (0.03%), $H_2^{18}O$ (0.20%), $HD^{16}O$ (0.0149%) and D_2O (0.0000022%) [12]. In our investigation, it is possible to observe all these isotopes with the exception of D_2O due to our spectrometer's detection limit of 3 ppm.

To determine the vibrational state we were making our rotational line measurements, we had to conduct an analysis on the available spectral and thermal energies in our experiment and compare it to water's fundamental frequencies. The fundamental frequencies for the three vibrational modes of water in the ground electronic state $X\ ^1A_1$ are $\nu_1 = 3657$ cm^{-1} (109.7 THz), $\nu_2 = 1594.7\ cm^{-1}$ (47.9 THz) and $\nu_3 = 3755.7\ cm^{-1}$ (112.7 THz) [13]. In our pulsed THz-TDS experiment we have a spectral range of 0.4 to 2.7 THz and an experimental temperature of 23.4 ^oC. Since our spectrometer's spectral range doesn't reach any of the fundamental vibrational modes and our translational energy at 23.4 ^oC is 308 cm^{-1}, we are restricted in making absorption measurements of rotational lines in the ground electronic ($X\ ^1A_1$), ground vibrational state (000) of water and its isotopes. This analysis describes that generally, most of the water lines measured are populated in the ground vibrational state. However, due to the complexity of the atmospheric constituents, there may be some excited vibrational states of water as well as magnetic dipole allowed transitions of diatomic oxygen. The complete analysis of the atmospheric spectrum is much to complex and beyond the scope of this paper.

Table 1 summarizes the seventy-two rotational lines measured where forty-nine of these resonances are $H_2{}^{16}O$, $X\ ^1A_1$ (000). The $H_2{}^{16}O$ lines measured in this investigation were validated by comparing the values to those obtained from the literature and they compared very well with the published lines within the 6.2 GHz resolution of our experiment. The center line frequencies we annotated for $H_2{}^{16}O$ were determined by comparing three atmospheric water vapor scans that were measured at different times in the year. The relative humidities of these scans ranged from 20 to 25 ± 2 %.

Conclusions

In this investigation, we conducted broadband absorption measurements of atmospheric water from 0.4 to 2.7 THz utilizing the THz-TDS technique. We measured a total of seventy-two lines. Forty-nine lines were identified as $H_2{}^{16}O$. All of our measured lines were within the 6.2 GHz resolution of the experiment when compared to previously measured or calculated lines in the literature. With this information, we have expanded the known spectral database of atmospheric water from 0.4 to 2.7 THz region. Also, we have provided the THz experimental community with a spectrum and a catalog of water lines to benchmark existing THz-TDS spectrometers. In addition, the experimental descriptions and figures in this paper provide the novice THz experimentalist with a means to build a ZnTe based THz-TDS spectrometer.

Table 1 Summary of measured lines. Forty-nine rotational transitions have been confirmed as $H_2{}^{16}O$, X^1A_1 (000), resonances. The resolution of our measured lines is 6.2 GHz.

This Work (THz)	Chen [a] (THz)	JPL [b] (THz)	Matsushima [c] (THz)	Exter [d] (THz)	Messer [e] (THz)	Kauppinen [f] (THz)
0.424						
0.436	0.437	0.437			0.437	
0.448	0.448	0.448			0.448	
0.479	0.475	0.475			0.475	
0.492	0.488	0.488			0.488	
0.504	0.504	0.504			0.504	
0.528	0.530	0.530				
0.559	0.557	0.557	0.557	0.557	0.557	
0.578	0.572	0.572				
0.596						
0.621	0.621	0.621			0.621	
0.645	0.646	0.646				
0.670						
0.688						
0.713						
0.737						
0.756	0.752	0.752	0.752	0.752	0.752	
0.799						
0.836	0.841	0.841				
0.891						
0.922	0.916	0.916	0.916		0.916	
0.934						
0.946						
0.965	0.970	0.970	0.970		0.970	
0.989		0.988	0.988	0.988	0.988	0.988
1.100	1.097	1.097	1.097	1.097		1.097
1.112	1.113	1.113	1.113	1.113		1.113
1.161	1.163	1.163	1.163	1.163		1.162
1.210	1.208	1.208	1.208	1.208		1.208
1.229	1.229	1.229	1.229	1.229		1.229
1.253						
1.302	1.308	1.308				
1.321	1.322	1.322	1.322			1.322
1.345	1.345	1.345				
1.376						
1.413	1.411	1.411	1.411	1.410		1.411
1.432						
1.518						
1.530						
1.542	1.542	1.542	1.542			1.542
1.604	1.602	1.602	1.602			1.602
1.665	1.661	1.661	1.661			1.661

Table 1. Continued

This Work (THz)	Chen [a] (THz)	JPL [b] (THz)	Matsushima [c] (THz)	Exter [d] (THz)	Messer [e] (THz)	Kauppinen [f] (THz)
1.720	1.717	1.717	1.717			1.717
1.763	1.762	1.762	1.762			1.762
1.800	1.797	1.797	1.797			1.797
1.868	1.868	1.868	1.868			1.868
1.923	1.919	1.919	1.919			1.919
1.941						
1.954						
1.997						
2.015	2.016	2.016	2.016			2.016
2.040	2.040	2.040	2.040			2.040
2.077	2.074	2.074	2.074			2.074
2.095						
2.163	2.164	2.164	2.164			2.164
2.199	2.196	2.196	2.196			2.196
2.224	2.222	2.222	2.222			2.222
2.267	2.264	2.264	2.264			2.264
2.298						
2.322	2.318	2.318	2.318			2.318
2.347	2.347	2.347	2.347			2.348
2.365	2.366	2.366	2.366			2.366
2.390	2.392	2.392	2.392			2.392
2.445	2.447	2.447	2.447			2.447
2.464	2.463	2.463	2.463			2.463
2.488						
2.525						
2.544						
2.568	2.567	2.567	2.567			2.567
2.642	2.640	2.640	2.640			2.640
2.666	2.665	2.665	2.665			2.665
2.684	2.686	2.686	2.686			2.686

[a] Reference 6
[b] Reference 14
[c] Reference 5
[d] Reference 4
[e] Reference 3
[f] Reference 2

References

[1] P.F. Bernath, *Phys. Chem. Chem. Phys*. 4 (2002) 1501-1509.

[2] J. Kauppinen, T. Karkkainen, E. Kyro, *J. Mol. Spec*. 71 (1978) 15-45.

[3] J.K. Messer, F.C. DeLucia, *Int. J. Infrared and Millimeter Waves* 4 (1983) 505–539.

[4] J.K. Messer, F.C. DeLucia, P. Helminger, *J. Mol. Spec* 105 (1984) 139-155.

[5] M.V.Exter, C. Fattinger, D. Grischkowsky, *Opt. Lett*. 14 (1989) 1128-1130.

[6] F. Matsushima, H. Odashima, T. Iwasaki, S. Tsunekawa, K. Takagi, *J. Mol. Struct.* 352/352 (1995) 371-378.

[7] F. Matsushima, H. Nagase, T. Nakauchi, H. Odashima, K. Takagi, *J. Mol. Spec*. 193 (1999) 217-223.

[8] P. Chen, J.C. Pearson, H.M. Pickett, S. Matsuura, G.A. Blake, *Astro. J. Supp. Series* 128 (2000) 371-385.

[9] P.Y. Han, X-C Zhang, *Meas. Sci. Technol*. 12 (2001) 1747-1756.

[10] A.N. Cox, *Allen's Astrophysical Quantities,* 4th ed., Springer-Verlag, New York, 2000, p. 258.

[11] C.H. Townes and A.L. Schawlow, *Microwave Spectroscopy*, Dover publication Inc, New York, 1975, p. 639.

[12] The relative isotopic water abundances are available on the World Wide Web at http://www.science.uwaterloo.ca/~cchieh/cact/applychem/waterchem.html, sponsored by the University of Waterloo, Department of Chemistry, Waterloo, Ontario, Canada.

[13] G. Herzberg, *Molecular Spectra and Molecular Structure Vol. III-Electronic Spectra and Electronic Structure of Polyatomic Molecules*, Krieger Publishing Company, Malabar, 1991, p. 585.

Distribution:

1	MS0603	Jim Hudgens, 1713
1	MS0603	Mike Wanke, 1713
1	MS0603	Igal Brener, 17131
1	MS0603	Mike Mangan, 1713
1	MS1153	Guillermo Loubriel, 5133
1	MS1153	Fred Zutavern, 5133
1	MS1153	Van Rudd, 5134
1	MS1423	Greg Hebner, 1128
1	MS1423	Rob Foltynowicz, 1128
1	MS1423	Ron Allman, 1128
1	MS0972	Andy Boye, 5710
1	MS0782	Chuck Rhykerd, 64182
1	MS1415	Mark Lee, 1123
1	MS1427	Julia Phillips, 1100
1	MS1421	Jerry Simmons, 1130
1	MS1415	Charles Barbour, 1120
1	MS9018	Central Technical Files, 8945-1
2	MS0899	Technical Library, 9616